Journal of Ovonic Research Vol. 15, No. 5, September - October 2019, p. 315 - 323

# SYNTHESIS, STRUCTURAL CHARACTERIZATION AND THERMOELECTRIC PROPERTIES OF $Sr_2(Sr_{n-1}Ti_nO_{3n+1})$ N-TYPE CERAMIC MATERIALS

T. RADHIKA[a,*], R. J. RAMALINGAM[b*], P. T. HASNA[a], A.M. TAWFEEK[b*], SHABAN R. M. SYED[b], H. AL-LOHEDAN[c], D. M. AL-DHAYAN[c]

[a]*Centre for Materials for Electronics Technology [C-MET, MeitY], Athani, Thrissur, Kerala, India.*

[b] *Chemistry Department, College of Science, King Saud University, Riyadh 11451, Saudi Arabia.*

[c]*Surfactants Research Chair, Chemistry Department, College of Science, King Saud University, Riyadh 11451, Saudi Arabia*

Ceramic oxide compositions based on R-P phases, $Sr_2(Sr_{n-1}Ti_nO_{3n+1})$; where n = 1,2 and 3 were prepared by solid-state reaction method. Materials with higher density could be obtained at higher calcination and sintering temperatures of 1573 K, 1623 K respectively. Formation of perovskite type $SrTiO_3$ and single phase R-P (Ruddlseden-Popper) phases were confirmed by X-ray diffraction pattern. The structural features were investigated in detail by various techniques such as TG-DSC, Raman and HR-TEM techniques. Electrical properties studied by Hall measurement set up with four probe method confirm the as prepared ceramics is n-type thermoelectric. Structural and electrical properties analysis shows that these ceramic oxide compositions are promising and potential catalyst for renewable thermo electric device applications

(Received January 14, 2019; Accepted October 4, 2019)

*Keywords:* Ruddlesden-Popper Phase, Thermoelectric, Hall measurement, $Sr_2(Sr_{n-1}Ti_nO_{3n+1})$

## 1. Introduction

The environmental impact of global climate change and world's demand for energy is becoming increasingly alarming. One way to improve the sustainability of our electricity base is through the utilization of waste heat. Thermoelectric materials, which can generate electricity from waste heat or be used as solid-state Peltier coolers, could play an important role in global sustainable energy solution [1]. Thermoelectric (TE) power generation converts dissipated heat generated by power stations, automobiles etc., into electrical energy and will play an important role in coming decades as an alternate energy technology [2-4]. The energy conversion efficiency of the TE power generation is governed by the dimensionless figure-of-merit, $ZT=S^2\sigma T/\kappa$ where, S, σ, κ and T are the Seebeck coefficient, electrical conductivity, thermal conductivity and absolute temperature, respectively. Materials with $ZT\approx1$ are considered high-performance with potential for commercial applications [5-7]. Oxide ceramics, show promise for TE power generation at high temperatures because the materials are generally nontoxic, inexpensive, and stable.

Recently $SrTiO_3$, an $ABO_3$ – type perovskite is identified as a potential candidate for n-type thermoelectric materials especially at high temperatures. However, its figure of merit (ZT) is far less than unity since it is having large thermal conductivity [8]. Recnetly, higher amount of Niobium (Nb)-doped strontium titanate, Nb-$SrTiO_3$, with perovskite-type structure is an n-type

*Corresponding author: jrajabathar@ksu.edu.sa

degenerate semiconductor and exhibits largest thermoelectric figure of merit (~ 0.37 at 1000 K) [9,10].

The compounds with general formulae $A_{n+1}B_nO_{3n+1}$ were first identified by Ruddlesden and Popper in 1957 and are termed as R-P compounds. Its structure is made up of n type perovskite layers sandwiched between an AO rock-salt type layers [11,12,]. The $Sr_2(Sr_{n-1}Ti_nO_{3n+1})$ phases are STO based Ruddlesden-Popper phase materials, where $Sr_2TiO_4$, $Sr_3Ti_2O_7$ and $Sr_4Ti_3O_{10}$ are represent the members for n=1, 2, 3 respectively, if n is infinity (∞), the compound is cubic perovskite-type $SrTiO_3$ [13]. The Ruddlesden-Popper phase SrO $(SrTiO_3)$n is a new TE materials, which have the possibility of exhibiting low k in the presence of Sr/$(SrTiO_3)$n interfaces. These oxides also have the potential to maintain the favorable electronic properties for TE materials, being built up with a sequence of one SrO layer intercalated between n$SrTiO_3$ perovskite layers [14]. The Ruddlesden-Popper phase material has the structure as embedding the electric conducting perovskite-blocks in between non conducting layers. The layered perovskite that is the insertion of SrO layers in between $SrTiO_3$ structure reduces the thermal conductivity K and hence increases the power factor $S^2\sigma T$ / K. In R-P phase the a-axis approximately equal to 3.90 Å for all compounds, while the c-axis increases from 13.71 to 20.3 to 28.1 Å as the numbers of perovskite blocks are increases from one to three. The RP series $Sr_2(Sr_{n-1}Ti_nO_{3n+1})$; where n=1,2 and 3 are interesting materials. Its structure is made up of n perovskite layers sandwiched between an AO rock-salt type layers. Because of the presence of SrO/$(SrTiO_3)$ interfaces, RP phase exhibits low thermal conductivity [15,16]. Characteristics of these materials make promising for TE applications [17].

Shibuya et al (2010), reported the simulation characteristics of $Sr_2TiO_4$ Thin Films for nanoswitches applications [18,19]. The rare earth metal ion doped strontium titanates has also tested for other renewable energy application such as solid oxide fuel cell electrodes, Ce-Doped La/Sr-Titanate [20-24]. In the present work, $SrTiO_3$ and R-P series ceramic oxide compositions were prepared by solid-state reaction method and its structural and electrical properties investigation was done in order to make use these materials for thermoelectric applications.

## 2. Experimental

### 2.1. Preparation of ceramic compositions

The ceramic oxide $SrTiO_3$ and R-P phase compositions were prepared through conventional solid-state reaction (SSR) method. The stoichiometric amounts of $SrCO_3$ (NICE Chemicals, 99%) and $TiO_2$ (MERCK, 99%) were mixed well in a mortar and the powder was subject to calcination (1073-1573 K, 6 h) followed by sintering (1373-1623 K, 3 h). The prepared powder is further fabricated in the form of pellets by mechanical pressing method.

#### *2.1.1. Preparation of $SrTiO_3$*

Strontium titanate (SrTiO3) was prepared by solid state method. Stoichiometric amounts of SrCO3 (NICE Chemicals, 99%) and TiO2 (MERCK, 99%) mixed well in a mortar. The powder was kept for calcination in a furnace at different temperature for 6 h.

The corresponding reaction is that,

$$SrCO_3+TiO_2 \rightarrow SrTiO_3+CO_2$$

Sintering was done at different temperature for 3 h after making pellets. Density was determined by calculation as well as Archimedes method.

#### *2.1.2. Preparation of R-P phases $Srn+1TinO_{3n+1}$*

The stoichiometric amounts of SrCO3 and TiO2 were mixed in a mortar. The corresponding reactions are,

$$aSrCO_3+bTiO_2 \rightarrow Sr_2TiO_4+2CO_2 \text{ (a=2,3,4 and b=1,2,3)}$$

$$3SrCO_3+2TiO_2 \rightarrow Sr_3Ti_2O_7+3CO_2 \ (n=2)$$
$$4SrCO_3+3TiO_2 \rightarrow Sr_4Ti_3O10+4CO_2 \ (n=3)$$

The powders were calcined at different temperatures and sintered after making pellets. Density was determined by calculation as well as Archimedes method.

**2.2. Structural and electrical properties investigation**

Bulk densities of the sintered materials were measured using Archimedes method. The powder X-Ray Diffraction (AXS Bruker D5005 X-ray diffractometer, Germany, 40 kV and 30 mA, CuKα (λ = 1.54 A°) radiation with Ni filter) was used to confirm the phase formation. The reflectance spectra were recorded on DR UV-Visible spectroscopy (Varian, Cary 5000). Raman spectroscopy (Thermo DXR Raman Microscope) was used to study the vibrational modes. Thermal data (TG-DSC) of the materials was obtained on SDT Q 600 V 8.3. Electrical properties such as bulk concentration, mobility, conductivity and average hall coefficient were measured at room temperature with fixed magnetic field of 0.54 T using four probe in ECOPIA HALL MEASURMENT SYSTEM (HMS-3000-VERS.51.5).

## 3. Results and discussion

In order to understand the weight changes during the preparation stage and thus the calcinations/sintering temperature, TG-DSC of the mixed powder was carried out (Fig. 1). General formula and weight loss during solid state preparation of $SrTiO_3$ and its corresponding RP phases are as follows.

$$SrCO_3+TiO_2 \rightarrow SrTiO_3+ CO_2 \uparrow (20.5\ \%),$$
$$3SrCO_3+2TiO_2 \rightarrow Sr_2TiO_4+ 3CO_2 \uparrow (24.3\ \%),$$
$$3SrCO_3+2TiO_2 \rightarrow Sr_3Ti_2O_7+ 3CO_2 \uparrow (22.7\ \%),$$
$$3SrCO_3+2TiO_2 \rightarrow Sr_4Ti_3O_{10}+ 3CO_2 \uparrow (22.0\ \%).$$

The theoretical weight loss for the formation of $SrTiO_3$ $Sr_2TiO_4$, $Sr_3Ti_2O_7$ and $Sr_4Ti_3O_{10}$ is 20.5, 24.3, 22.7, 22.0 (%) respectively. From the thermal patterns, it is clear that, the complete formation of phase pure material occurs in the temperature range higher than 1273 K with the elimination of $CO_2$. Thus the calcinations temperature higher than 1273 K was selected in order to establish formation of highly dense ceramic compositions.

The powder X-ray diffraction of all the materials was recorded at various calcinations temperature. The XRD of $SrTiO_3$ is shown in Fig. 2. For the composition calcined at 1473 K, the pattern shows all the peaks corresponding to $SrTiO_3$ as compared with the JCPDS file no 00-035-0734. The $SrTiO_3$ forms pure perovskite phase with (110) as the most intense peak. Highly crystalline pattern is observed when the calcinations temperature is increased to 1573 K. The powder X-ray diffraction pattern of $SrTiO_3$ shows that at higher calcinations temperatures (1273-1573 K) the formation of phase pure $SrTiO_3$ is occur with major intense peak (110). Phase formation is compared and confirmed with JCPDS file 00-035-0734. Lattice parameters calculated from powder X-ray diffraction using miller indices $d_{hkl}$ values are a=b=c = 3.9 (A˚), the lattice parameters observed for $SrTiO_3$ is a=b=c=3.9 (A˚) since it is cubic. The powder X-ray diffraction of the $Sr_2TiO_4$ calcined at different temperatures was recorded and is shown in Fig. 3.

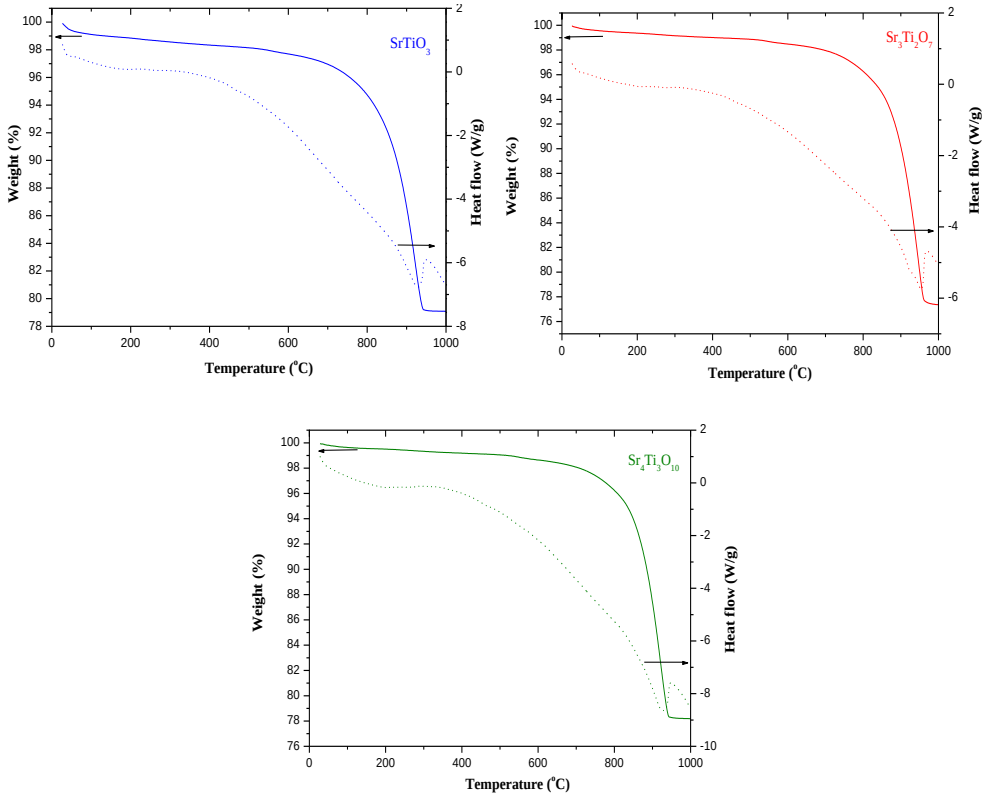


*Fig. 1. TG-DSC pattern of different composition of Strontium titanate ceramics.*

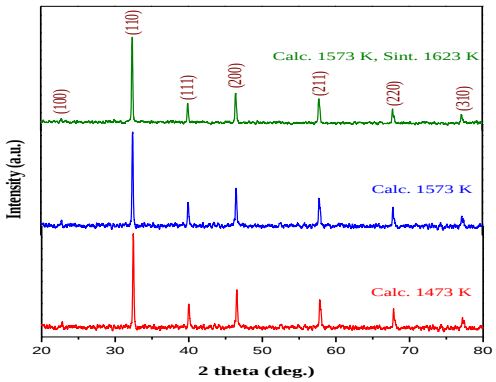


*Fig. 2. XRD patterns of $SrTiO_3$ calcined at various temperatures.*

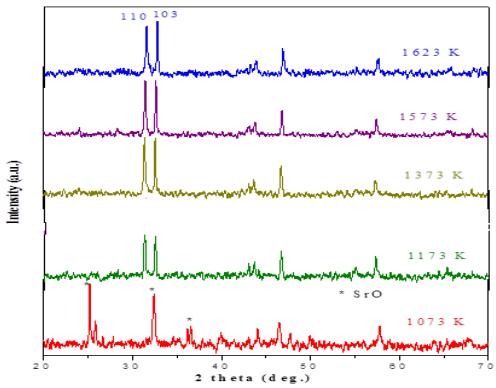


*Fig. 3. X-ray diffraction pattern of $Sr_2TiO_4$ calcined at various temperatures.*

In the case of $Sr_2TiO_4$ pure phase formation occurs with different ratio of most intense peaks (110) and (103). The powder X-ray diffraction pattern of $Sr_2TiO_4$ shows that at calcinations temperature of 1073 K, the material is not formed. However, at higher calcinations temperatures (1173-1573 K) the formation of pure phase $TiO_4$ is occurs but with different ratio (~100-54, 100:99.9 etc.) with major intense peaks appeared at (110) and (103). Phase formation is compared and confirmed with JCPDS file 00-039-1471. The lattice parameters and intensity ratio of $Sr_2TiO_4$ calculated from powder X-ray diffraction data. The lattice structure of $Sr_2TiO_4$ is body centered tetragonal. Thus the lattice parameters a=b≠c. The lattice parameters a=b and c of $Sr_2TiO_4$ obtained using d space values and $d_{hkl}$ are ~ 3.87-3.88 (A˚) and 12.48-12.58 (A˚). These are comparable with theoretical values of 3.88 A˚ and 12.59 A˚ respectively [25,26].

Phase pure $Sr_3Ti_2O_7$ is formed with maximum intense peaks as (110) and (105) in the ratio of (100:82). The powder X-ray diffraction pattern of $Sr_3Ti_2O_7$ shows that at higher calcinations temperatures (1273-1573 K) results in the formation of phase pure $Sr_3Ti_2O_7$ is occurs but with different ratio (~75.4:100, 100:82.5etc.) of maximum intense peaks (110) and (105). The Phase formation is compared with other method prepared same materials and confirmed with JCPDS file 9-4-2075.

Lattice parameters and intensity ratio of $Sr_3Ti_2O_7$ calculated from powder X-ray diffraction data (not shown). The lattice structure of $Sr_3Ti_2O_7$ is body centered tetragonal. Thus the lattice parameters a=b≠c. The lattice parameters a=b and c of $Sr_3Ti_2O_7$ obtained are ~ 3.87-3.89 (A˚) and 20.18-20.36 (A˚). These are comparable with theoretical values of 3.90 A˚ and 20.38 A˚ respectively.

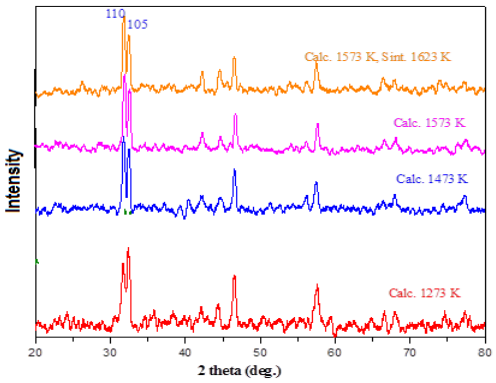


*Fig. 4. X-ray diffraction pattern of $Sr_3Ti_2O_7$ calcined at various temperatures.*

At 1573 K, the pattern shows all the peaks corresponding to $Sr_4Ti_3O_{10}$ with ratio of 63.4:100. The powder X-ray diffraction pattern of $Sr_4Ti_3O_{10}$ shows that at higher calcinations temperatures (1273-1573 K) the formation of phase pure $Sr_4Ti_3O_{10}$ is occur but with different ratio (~56:100, 63.4:100etc.) of maximum intense peaks (110) and (107). Phase formation is compared and confirmed with JCPDS file 00-022-1444. Lattice parameters and intensity ratio of $Sr_4Ti_3O_{10}$ calculated from powder X-ray diffraction data.

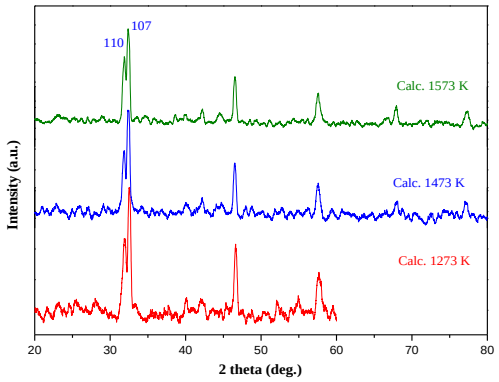


*Fig. 5. X-ray diffraction pattern of $Sr_4Ti_3O_{10}$ calcined at various temperatures.*

The lattice structure of $Sr_4Ti_3O_{10}$ is body centered tetragonal. Thus the lattice parameters a=b≠c. The lattice parameters a, b and c of $Sr_4Ti_3O_{10}$ obtained are ~ 3.88-3.89 (A˚) and 28.04-28.44 (A˚). These are comparable with theoretical values of 3.90 A˚ and 28.14 A˚ respectively. Phase pure $Sr_4Ti_3O_{10}$ is formed with maximum intense peaks as (110) and (107) respectively. The $Sr_2TiO_4$, $Sr_3Ti_2O_7$ and $Sr_4Ti_3O_{10}$ are body centered tetragonal in structure and thus the parameters a=b≠c.

The Raman spectra of the materials were recorded to study the structural dynamics and are shown in Fig. 6. The Raman spectrum of a $SrTiO_3$ is second order Raman – scattering. The optical phonons in bulk $SrTiO_3$ are Raman inactive due to crystal symmetry. The shifts observed in Raman spectrum of $SrTiO_3$ ceramics could due to the presence of defects in its structure. The Raman spectrum is perfectly matching with theoretical spectrum. Thus it suggests that the dynamical properties of prepared $SrTiO_3$ are perfect. The observed Raman modes are four (2 $A_{1g}$ and 2 $E_g$ modes) for $Sr_2TiO_4$, ten (4 $A_{1g}$, 1 $B_{2g}$ and 5 $E_g$ modes) for $Sr_3Ti_2O_7$ and fourteen (6 $A_{1g}$, 1 $B_{1g}$ and 7 $E_g$ modes) for $Sr_4Ti_3O_{10}$. The $A_{1g}$ modes correspond to symmetric stretch of the oxygen lattice corresponding in the $TiO_6$ octahedra. The obtained Raman spectra clearly confirm the formation of phase pure layered R-P phase ceramics. The space group of $Sr_2TiO_4$ is D17 4h**.** The spectrum gives strong bands in the range of 500-700 $cm^{-1}$. A single strong band is appears at 579 $cm^{-1}$. The spectrum confirms the formation of phase pure $Sr_2TiO_4$ as confirmed by X-ray diffraction pattern as well as by XRD by purity of crystallinity of the synthesized samples. The spectrum of $Sr_3Ti_2O_7$ gives strong bands in the range of 500-700 $cm^{-1}$. A single strong band is appears at 175 $cm^{-1}$. The spectrum confirms the formation of pure phase formation for $Sr_3Ti_2O_7$ as confirmed by X-ray diffraction pattern. Fourteen Raman modes (six $A_{1g}$, one $B_{1g}$and seven $E_g$ modes) are expected for $Sr_4Ti_3O_{10}$. The spectrum gives strong bands in the range of 500-700 $cm^{-1}$. A single strong band is appears at 180 $cm^{-1}$. The spectrum confirms the formation of phase pure $Sr_4Ti_3O_{10}$ as confirmed by X-ray diffraction pattern. The Raman spectra of prepared samples match with theoretical pattern. The maximum intense peaks are observed at 180 $cm^{-1}$ and 497 $cm^{-1}$ as shown in the Fig. 6. The TE micrograph (Fig.7) of $Sr_2TiO_4$ shows the formation of nanorods and fine spherical aggregated particle formation on layered arrangements of oxide matrixes and it appeard in the form of layered structure for R-P phase of strontium titanate based ceramic oxide. This layered structure made up by the insertion of SrO (Rock-salt) in between $SrTiO_3$ perovskite structure. The EDAX shows the presence of Sr and Ti in the R-P phase. The weight percentage of Oxygen (56%), Strontium (28%) and Titanium (16%) for $Sr_2TiO_4$.

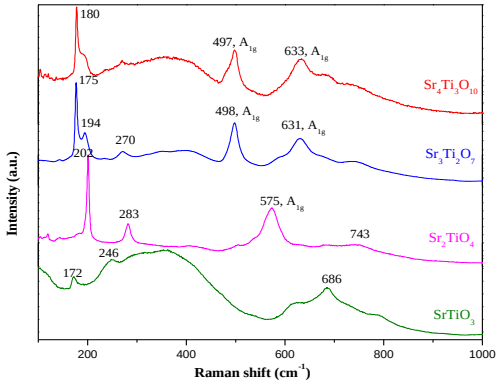


*Fig. 6. Raman spectra of the different composition of Strontium titanate ceramics.*

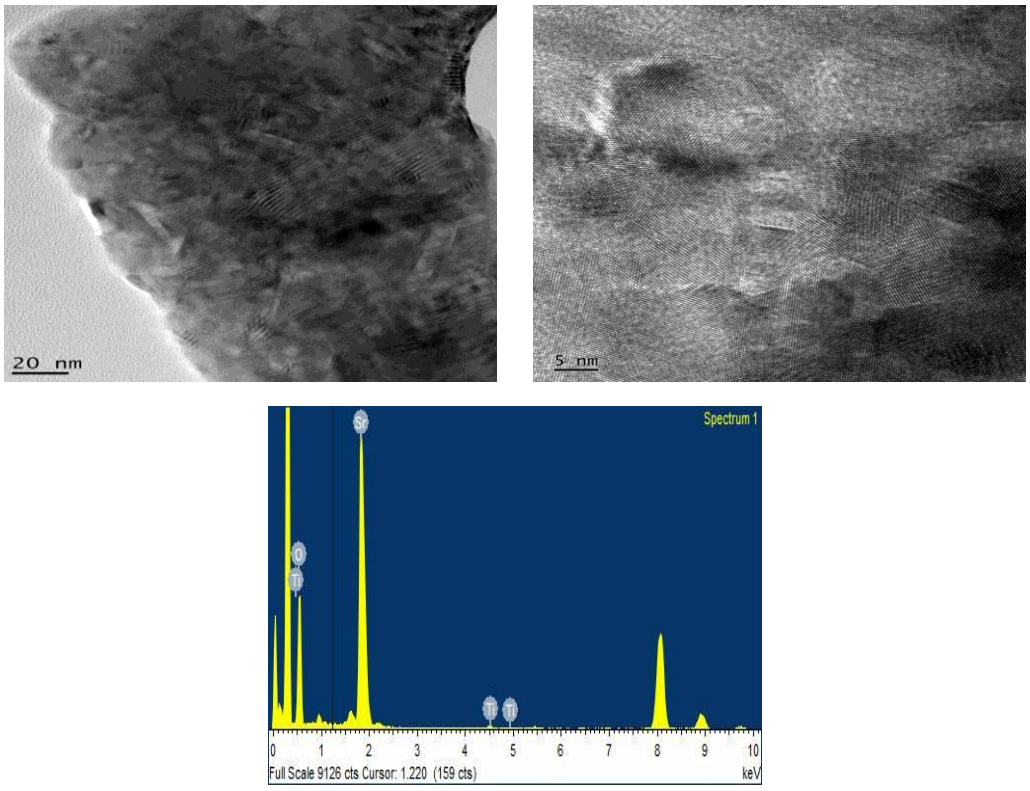


*Fig. 7. High resolution Transmission Electron micrographs of $Sr_2TiO_4$ and EDAX*

The electrical properties of the materials sintered at 1623 K were measured using Hall measurement set up with four probe method and is presented in Table 1. From the Hall measurement, it is confirmed that the prepared ceramic oxide compositions are n-type materials since the carrier concentration and Hall coefficient appears negative. Carrier concentration increased for R-P phases and is in the order of $10^{11}$ $cm^{-3}$. Decrease in resistivity and thus an increase in conductivity is observed for R-P phases compared to $SrTiO_3$ perovskite. Improved properties of R-P phases suggest its application towards thermo electric device fabrication.

**Table 1.** Electrical properties from Hall measurement

| Material | Carrier concentration ($cm^{-3}$) | Mobility ($cm^2V^{-1}s^{-1}$) | Resistivity ($\Omega cm$)*$10^6$ | Conductivity ($1/\Omega cm$)*$10^{-7}$ | Hall coefficient ($cm^3/C$) |
|---|---|---|---|---|---|
| $SrTiO_3$ | -8.62*$10^9$ | 1.84*$10^2$ | 3.94 | 2.54 | -7.24*$10^8$ |
| $Sr_2TiO_4$ | -4.43*$10^{11}$ | 5.64 | 2.49 | 4.01 | -1.41*$10^7$ |
| $Sr_3Ti_2O_7$ | -1.81*$10^{11}$ | 11.55 | 2.97 | 3.36 | -5.63*$10^7$ |
| $Sr_4Ti_3O_{10}$ | -1.81*$10^{11}$ | 11.55 | 2.97 | 3.36 | -5.63*$10^7$ |

## 4. Conclusions

The perovskite type $SrTiO_3$, Ruddlesden-Popper series such as $Sr_2TiO_4$, $Sr_3Ti_2O_7$ and $Sr_4Ti_3O_{10}$ were formed with single phase with high density particles with good crystallinity by solid state reaction method. The pure phase formation was confirmed by XRD and Raman spectroscopy. TEM images revealed that the formation of nanorods and fine spherical aggregated particle formation on layered arrangement of oxide matrixes. Thermal conductivities and electrical properties are explained in characterized by Hall measurement and it's confirmed as n-type ceramics formation. Improved electrical properties such as carrier concentration, resistivity is obtained and it could be the promising ceramic materials for thermoelectric based device fabrication.

**Acknowledgement**

The authors are grateful to the King Saud University for all financial support and to the Deanship of Scientific Research, College of Sciences, Research Center.

## References

[1] S. Ohta, H. Ohta, K. Koumoto, J. European Ceram. Soc. **2003**(23), 2639 (2003).
[2] G. J. Snyder, E. S. Toberer, Nature Materials **7**, 105 (2008).
[3] T. Hungria, Ana-Belen Hungria, A. Castro, J. Solid State Chem. **177**, 1559 (2004).
[4] T. Hungria, J. G. Lisoni, A. Castro, J. Chem. Mater. **14**, 1747 (2002).
[5] H. Y. He, W. P. Lao, J. F. Huang, J. Ceram. Process. Res. **11**, 485 (2010).
[6] C. Navas, Z. I. Hans-Conrad, J. Solid State Ionics **93**, 171 (1997).
[7] L. Zhang, Tsuyoshi, N. Okinaka, T. Akiyama, J. Mater. Trans. **48**, 1079 (2007).
[8] S. Ohta, T. Nomura, H. Ohta, K. Koumoto, J. Appl. Phys. **97**, 034106 (2005).
[9] S. Ohta, T. Nomura, H. Ohta, K. Koumoto, J. Appl. Phys. Lett. **87**, 092108 (2005).
[10] S. Ohta, T. Nomura, H. Ohta, K. Koumoto, J. Ceram. Soc. Jpn. **114**, 102 (2006).
[11] S. N. Ruddelesden, P. Popper, Acta Cryst. **10**, 538 (1957).
[12] S. N Ruddelesden, P. Popper, Acta Cryst. **11**, 54 (1958).
[13] K. Koumoto, Proc. 23rd Int. Conf. Thermoelectrics, IEEE, Piscataway 92 (2005).
[14] F. Gao, S. Yang, J. Li, M. Qin, Y. Zhang, H. Sun, J. Ceram. Inter. **41**, 127 (2015).

[15] A. Kikusi, L. Zhang, N. Okinaka, T. Tosho, T. Akiyama, J. Mater. Trans. **11**, 2675 (2009).
[16] S. Kamba, P. Samoukina, F. Kadlec, J. Pokorny, J. Petzelt, I. M. Reaney, P. L. Wise, J. Euro. Ceram. Soc. **23**, 2639 (2003).
[17] P. Affez, G. Tendeloo, R. Seshadri, M. Hervieu, C. Martin, A. Maignan, B. Raveau, J. Appl. Phys. **80**, 5850 (1996).
[18] K. Shibuya, R. Dittmann, S. Mi, R. Waser, Adv. Mater. **22**(3), 411–4 (2010).
[19] Amr H. H. Ramadan, Neil L. Allan, Roger A. De Souza, J. Am. Ceram. Soc. **96**(7), 2316 (2013).
[20] C. Perillat-Merceroz, G. Gauthier, P. Roussel, Chem. Mater. **23**, 1539 (2011).
[22] Liangliang Li, Ruirui Sun, Xiaoying Qin, Yongfei Liu, Guanglei Guo, Materials Science Forum **743-744**, 94 (2013).
[23] A. Kikuchi, N. Okinaka, T. Akiyama, Scr. Mater. **63**, 407 (2010).
[24] Y. F. Wang, K. H. Lee, H. Ohta, K. Kournoto, Ceram. Int. **34**, 849 (2008).
[25] K. T. Jacob, G. Ragitha, J. Chem. Thermodynamics **43**, 51 (2011).
[26] M. M. Elcombe, E. H. Kisi, K. D. Hawkins, T. J. White, P. Goodman, S. Matheson, Acta Cryst. **B47** 305 (1991).